Resilience of steel moment-frame buildings with reserve lateral strength

Johnn P. Judd and Finley A. Charney
Virginia Tech
Department of Civil and Environmental Engineering
Blacksburg, Virginia

15th U.S.-Japan Workshop on the Improvement of Structural Engineering and Resiliency, December 3-5, 2014, Big Island of Hawaii

Archetype building layout

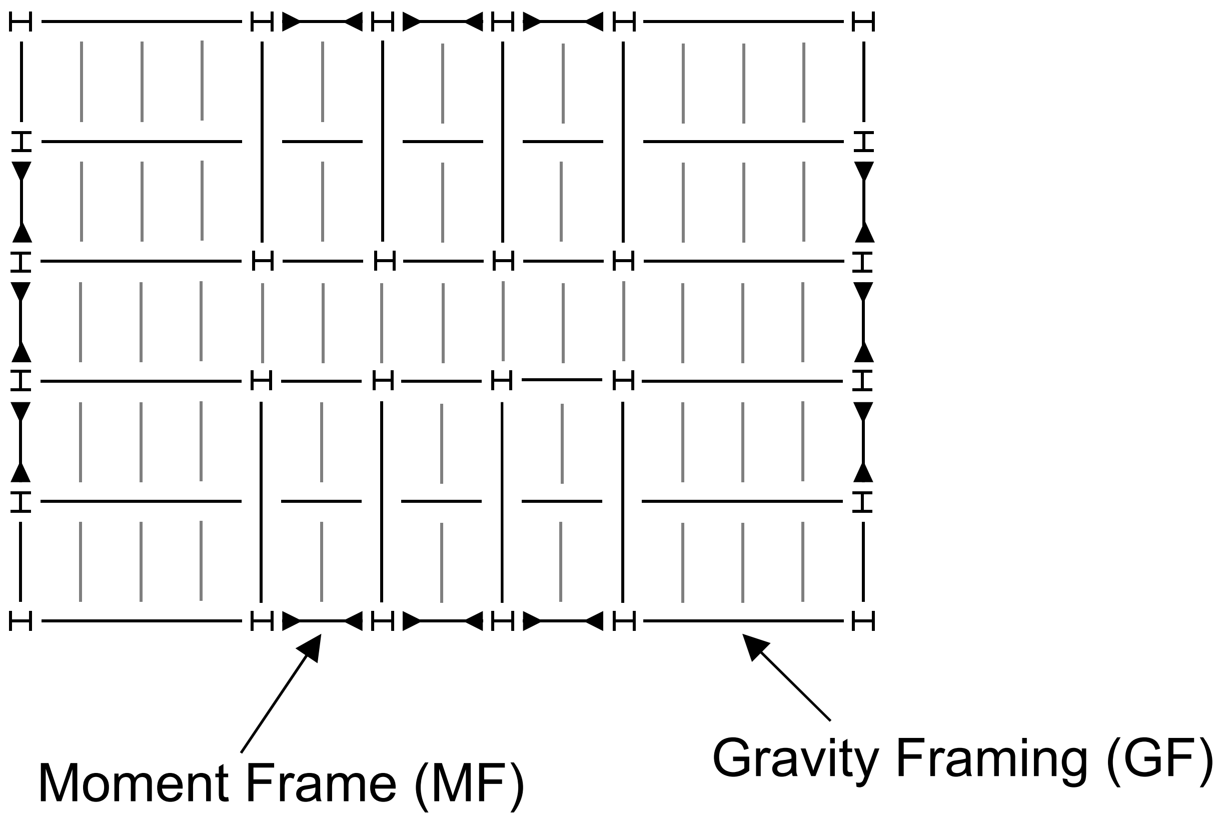

Archetype buildings

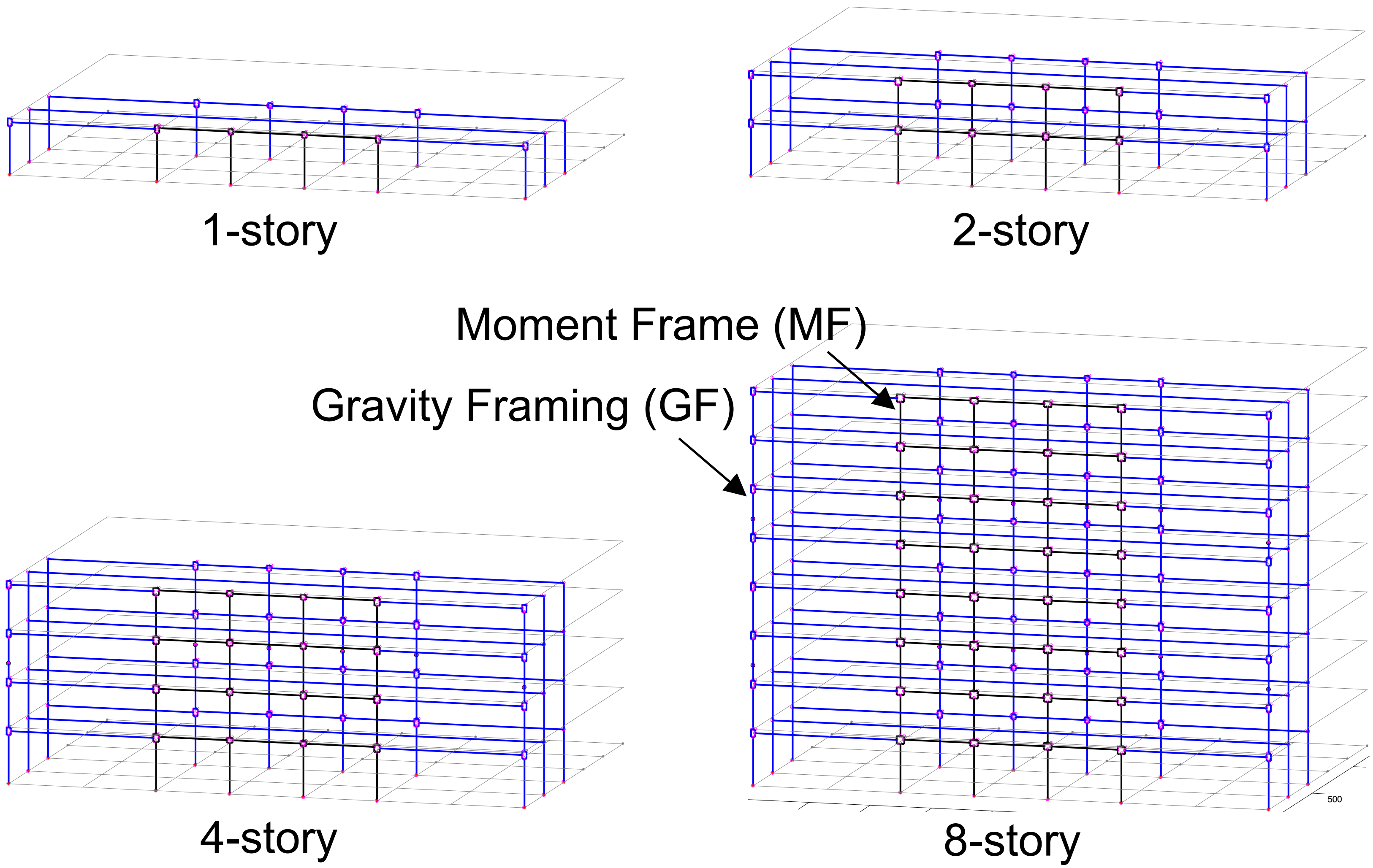

Lateral-force resisting system

Non-Ductile Moment Frame with beam-to-column connections not specifically detailed for seismic resistance.

- Element: `zeroLength`
- Behavior: `Pinching4`, `MinMax` with envelope/hysteresis parameters based on FEMA P-440A, ASCE 41, and FEMA 355D.

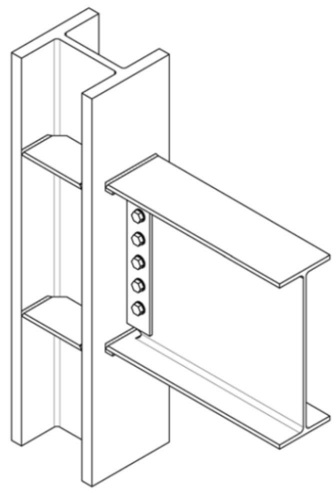

(from Hamburger et al. 2009)

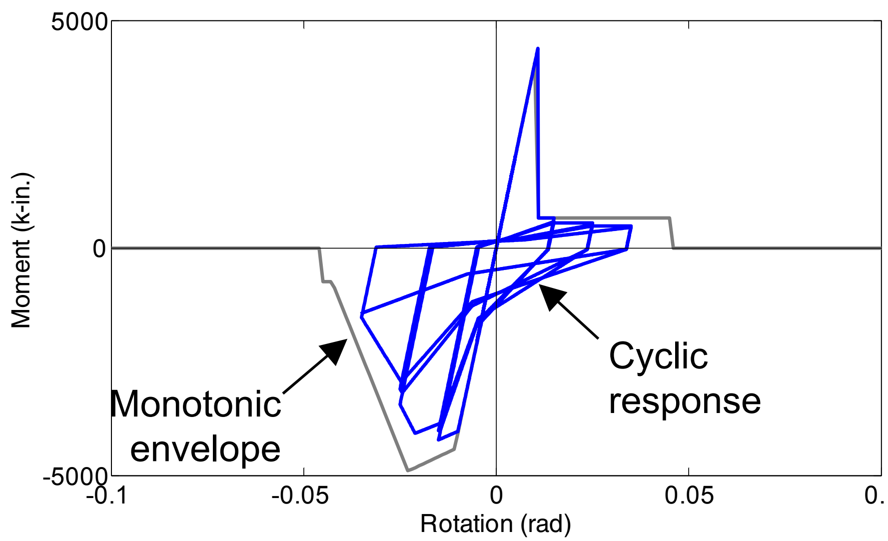

Lateral-force resisting system

Ductile Special Moment Frame (SMF) designed for Seismic Design Category (SDC) D_{min} or SDC D_{max}.

- Element: `zeroLength`
- Behavior: `Bilin` with envelope/hysteresis parameters based on regression analysis of NEES database (Lignos and Krawinkler 2011)

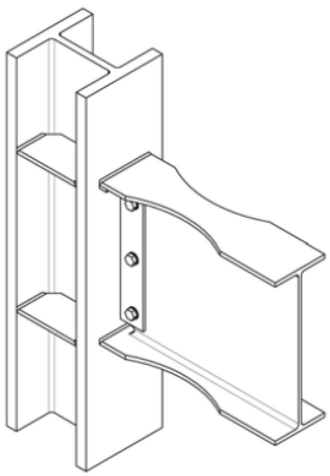

(from Hamburger et al. 2009)

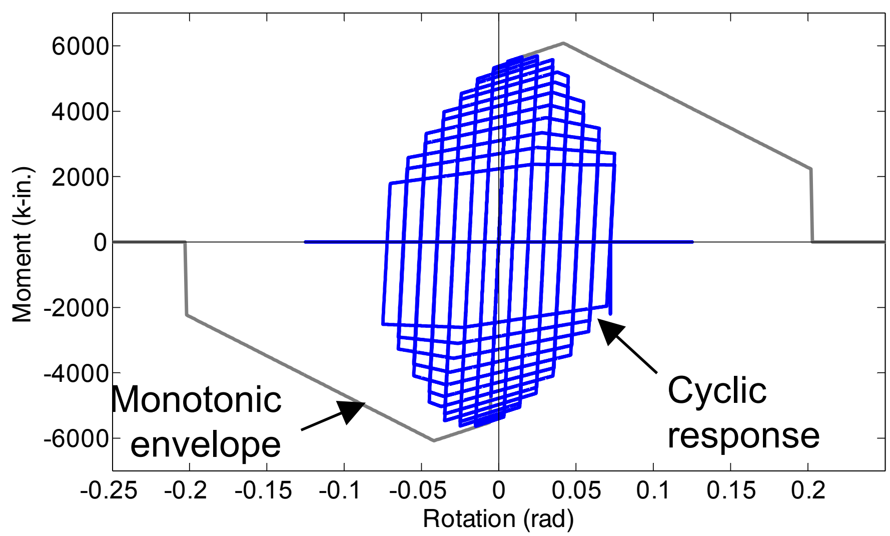

Gravity framing system

Shear tab beam-to-column connection.

- Element: `zeroLength`
- Behavior: `Pinching4`, `MinMax` with envelope/hysteresis parameters based on test data (Liu Astaneh-Asl 2000) and corresponding analytical models (Liu Astaneh-Asl 2000; Wen and Shen 2013).

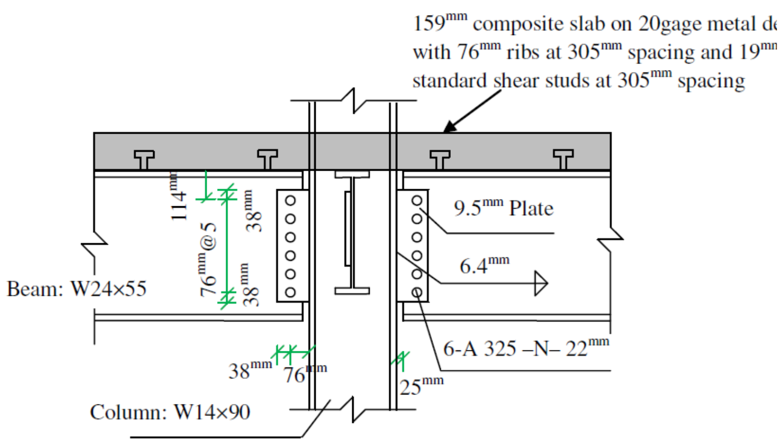

(from JCSR, Wen et al. 2013)

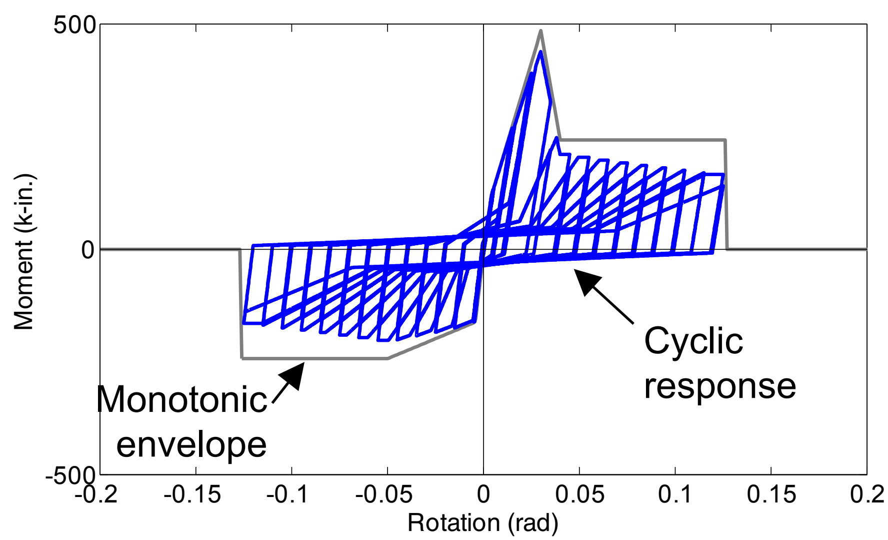

Performance assessment

Serviceability: Western United States

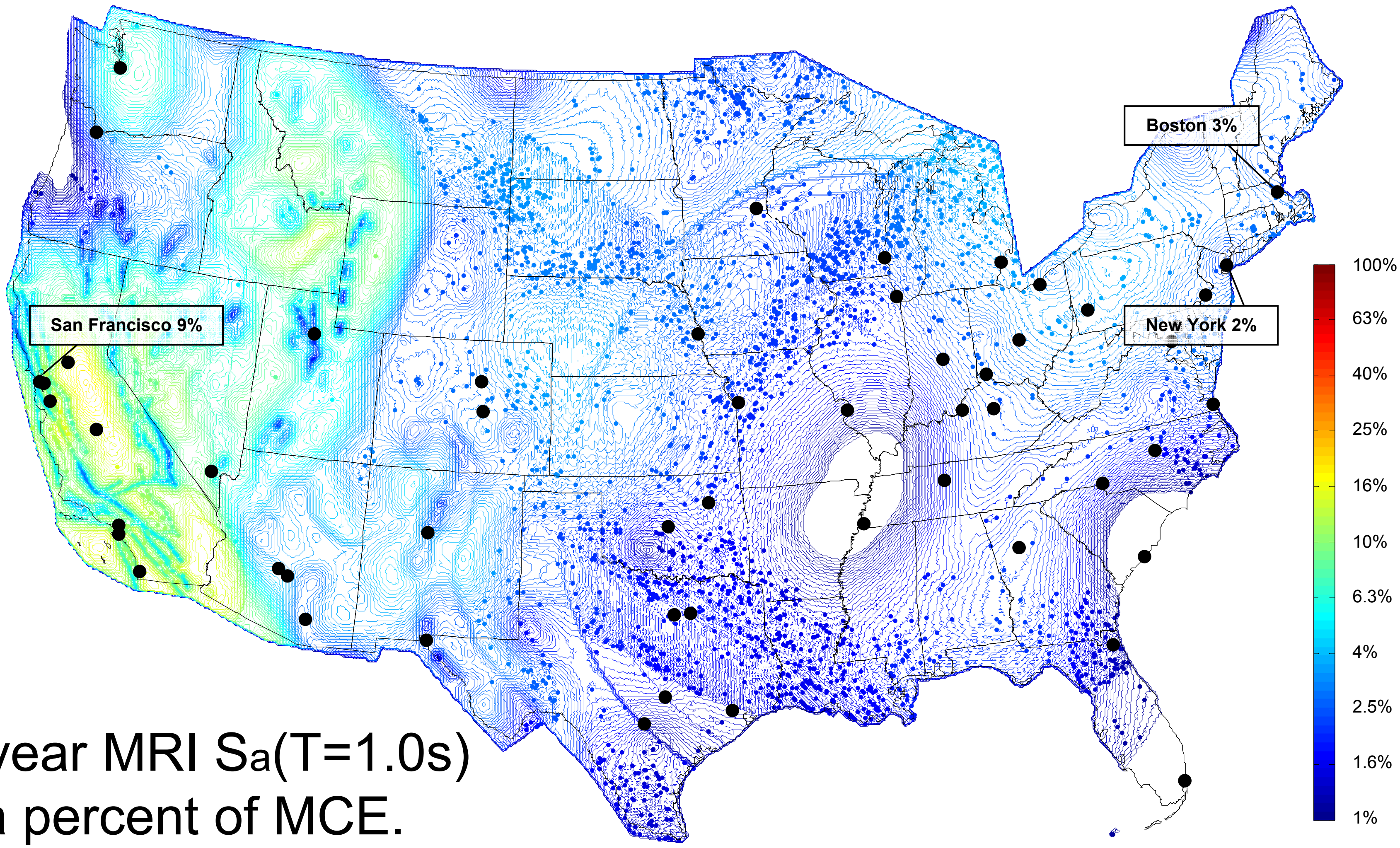

25-year MRI $S_a(T=1.0s)$ as a percent of MCE.

Performance assessment

Serviceability: Central and Eastern United States

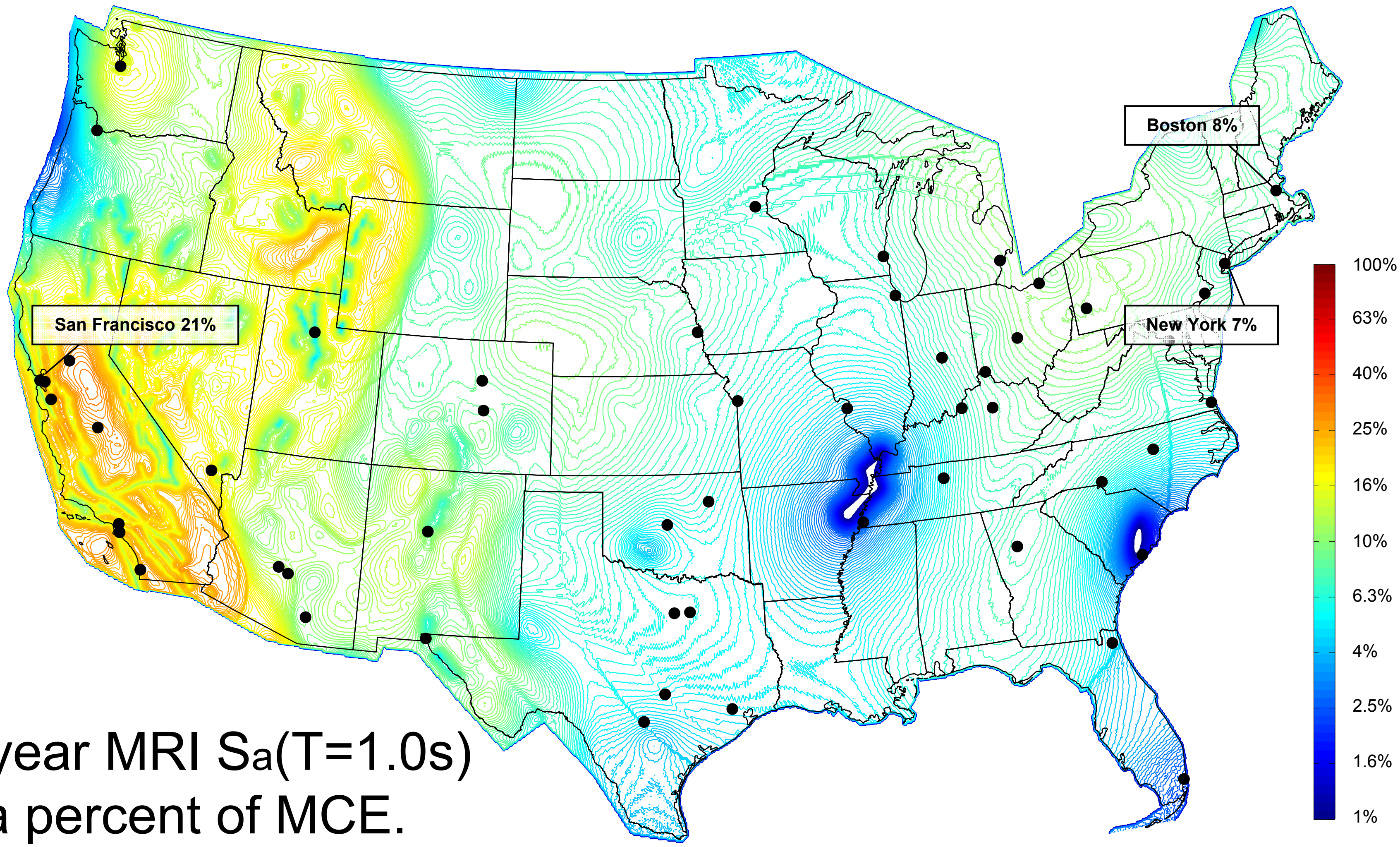

72-year MRI $S_a(T=1.0s)$
as a percent of MCE.

Serviceability-level performance

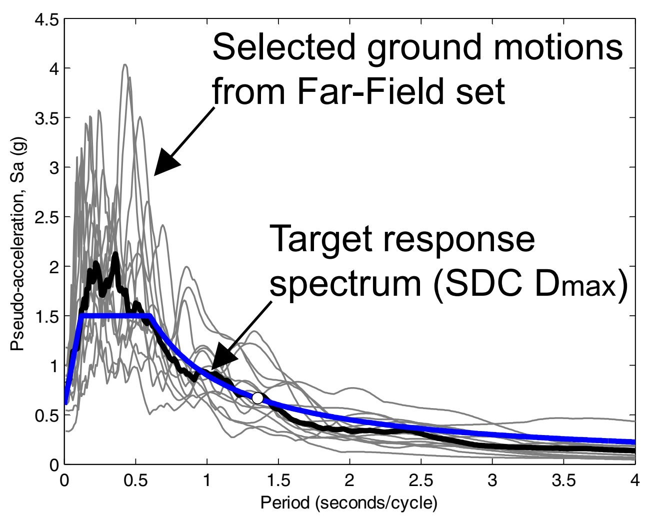

Response spectrum: 4-story

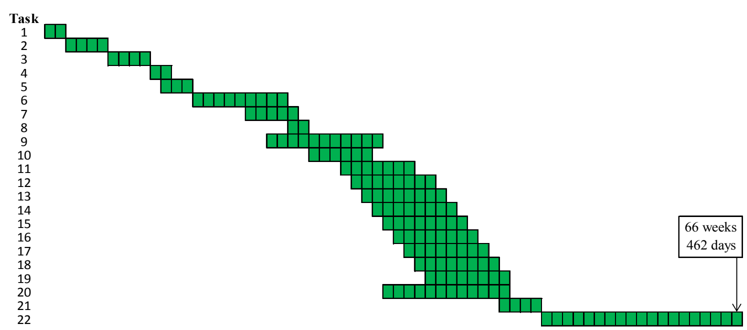

Construction Schedule: 4-story
(from Jarrett et al. 2015)

Component Fragilities

Component Description (FEMA P-58 Fragility ID)		Quantity	Demand Parameter
Structural Components			
Beam-to-column connections	Non-ductile, Pre-Northridge WUF-B, single sided (B1035.041)	4	IDR
	Non-ductile, Pre-Northridge WUF-B, double sided (B1035.051)	4	IDR
	Ductile, Post-Northridge RBS, single sided (B1035)	4	IDR
	Ductile, Post-Northridge RBS, double sided (B1035)	4	IDR
	Gravity frame, bolted shear tab (B1031.001)	32	IDR
Moment frame columns	Column base plates (B1031)	8	IDR
	Column splices, welded (B1031)	8	IDR
Non-Structural Components			
All stories	Curtain Walls (B2022.001)	4,200 sf	IDR
	Wall Partition (C1011.001a)	1,400 lf	IDR
	Prefabricated steel stair (C2011.001b)	2 ea	IDR
	Wall Partition (C3011.001a)	106 lf	IDR
	Raised Access Floor (C3027.001)	10,500 sf	Acceleration
	Suspended Ceiling (C3032.001a)	12,600 sf	Acceleration
	Independent Pendant Lighting (C3034.001)	210 ea	Acceleration
	Cold Water Piping (D2021.011a)	210 lf	Acceleration
	HVAC Metal Ducting (D3041.011a)	1,050 lf	Acceleration
	HVAC Metal Ducting (D3041.012a)	280 lf	Acceleration
	HVAC Drops (D3041.031a)	126 ea	Acceleration
	(VAV) box (D3041.041a)	98 ea	Acceleration
	Fire Sprinkler Water Piping (D4011.021a)	2,800 lf	Acceleration
	Fire Sprinkler Drop (D4011.031a)	126 ea	Acceleration
	Low Voltage Switchgear (D5012.021a)	225 ea	Acceleration
1st story	Traction Elevator (D1014.011)	4 ea	Acceleration
Roof	Chiller (D3031.011a)	360 tn/ea	Acceleration
	Cooling Tower (D3031.021a)	360 tn/ea	Acceleration
	Air Handling Unit (D3052.011a)	88,200 cf	Acceleration
	Motor Control Center (D5012.013a)	6 ea	Acceleration

Quantification of resilience

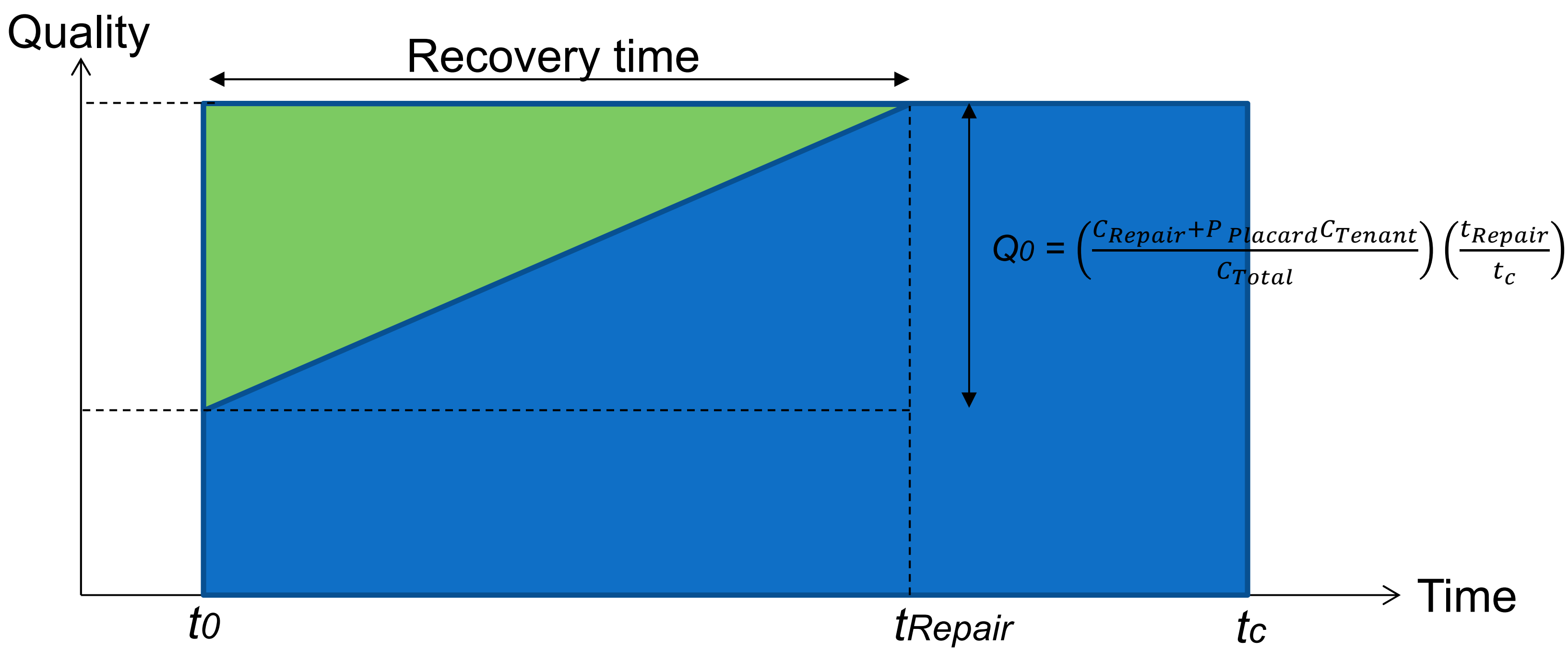

$$R = \int_{t_0}^{t_c} [1 - Q(t)]dt$$

$$= 1 - \frac{1}{2}\left(\frac{C_{Repair} + P_{Placard}C_{Tenant}}{C_{Total}}\right)\left(\frac{t_{Repair}}{t_c}\right)$$

Serviceability-level performance

Non-ductile Moment Frame

Archetype	Repair		Prob. of Unsafe Placards	Resilience
	Cost ($)	Time (days)		
1-story				
MF	277,500	50	0.49	0.79
MF+GF	220,000	32	0.26	0.92
2-story				
MF	330,000	36	0.21	0.93
MF+GF	266,250	32	0.15	0.95
4-story				
MF	666,667	40	0.19	0.93
MF+GF	490,000	27	0.09	0.97
8-story				
MF	1,192,000	48	0.10	0.94
MF+GF	775,000	29	0.03	0.99

Serviceability-level performance

SMF Designed for SDC D_{min}

Archetype	Repair Cost ($)	Repair Time (days)	Prob. of Unsafe Placards	Resilience
1-story				
MF	237,273	43	0.46	0.83
MF+GF	216,667	31	0.21	0.94
2-story				
MF	340,000	31	0.18	0.94
MF+GF	275,556	27	0.12	0.97
4-story				
MF	620,000	28	0.05	0.98
MF+GF	577,143	26	0.03	0.98
8-story				
MF	1,120,000	37	0.09	0.96
MF+GF	870,000	29	0.03	0.98

Serviceability-level performance

SMF Designed for SDC D_{min}

Archetype	Repair		Prob. of Unsafe Placards	Resilience
	Cost ($)	Time (days)		
1-story				
MF	237,273	43	0.46	0.83
MF+GF	216,667	31	0.21	0.94
2-story				
MF	340,000	31	0.18	0.94
MF+GF	275,556	27	0.12	0.97
4-story				
MF	620,000	28	0.05	0.98
MF+GF	577,143	26	0.03	0.98
8-story				
MF	1,120,000	37	0.09	0.96
MF+GF	870,000	29	0.03	0.98

Serviceability-level performance

8-story SMF Designed for SDC D_{min}

- **Repair Costs**: Most repair costs were caused by damage to the gypsum wall partitions. The reserve lateral strength from the gravity framing reduced repair costs by 22%.

- **Repair Time**: The time required for repairs is correlated to repair costs, and was dominated by repair time for the gypsum wall partitions. Interestingly, including the gravity framing actually increased the probable repair time for some components (chiller).

Serviceability-level performance

8-story SMF Designed for SDC Dmin

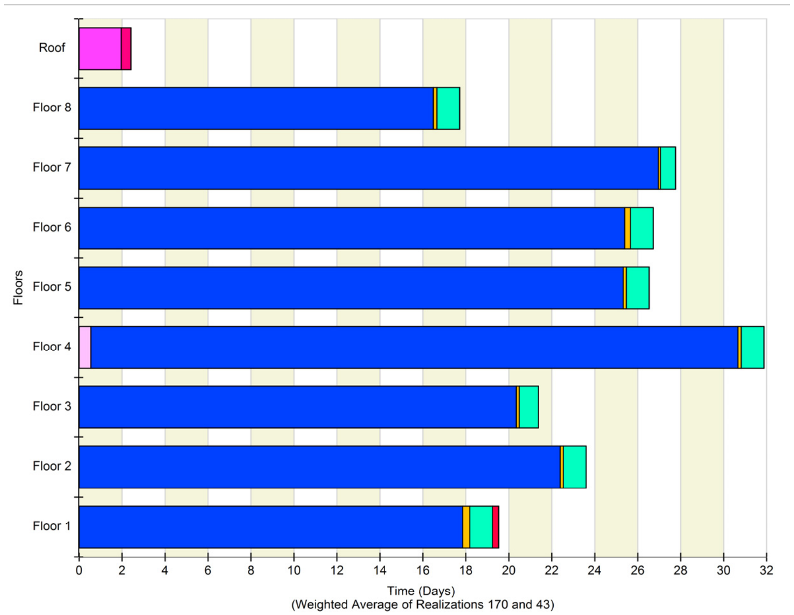

Moment frame only (MF)

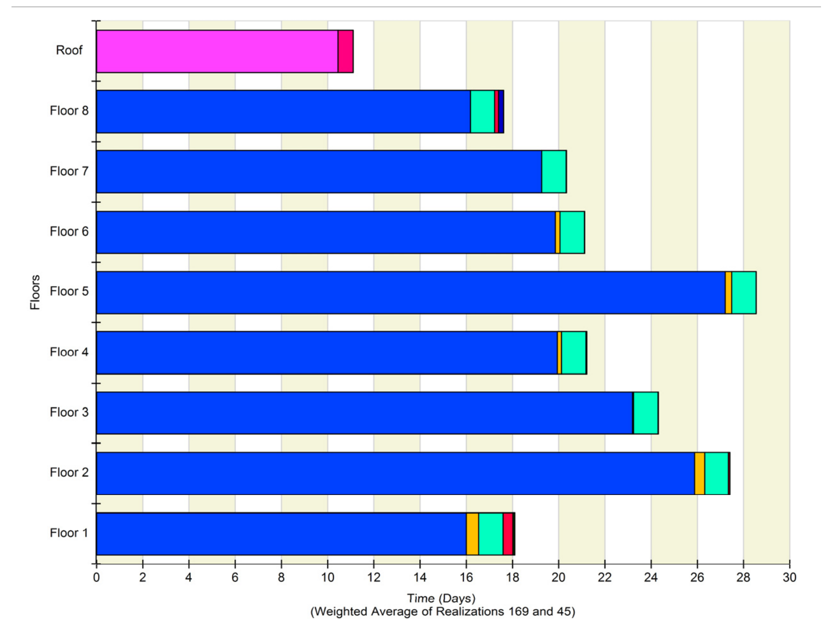

With reserve strength (MF+GF)

Serviceability-level performance

8-story SMF Designed for SDC D_{min}

- **Repair Costs**: Most repair costs were caused by damage to the gypsum wall partitions. The reserve lateral strength from the gravity framing reduced repair costs by 22%.

- **Repair Time**: The time required for repairs is correlated to repair costs, and was dominated by repair time for the gypsum wall partitions. Interestingly, including the gravity framing actually increased the probable repair time for some components (chiller).

- **Unsafe placards**: Placarding was caused due to prefabricated steel stair systems with steel treads and landings without seismic joints. Reserve strength reduced this from 9% to 3%.

Serviceability-level performance

SMF Designed for SDC D_{max}

Archetype	Repair		Prob. of Unsafe Placards	Resilience
	Cost ($)	Time (days)		
1-story				
MF	315,000	24	0.06	0.97
MF+GF	288,000	23	0.05	0.97
2-story				
MF	362,222	20	0.03	0.98
MF+GF	300,000	18	0.03	0.99
4-story				
MF	577,143	26	0.03	0.98
MF+GF	490,000	24	0.05	0.98
8-story				
MF	767,500	25	0.01	0.99
MF+GF	642,000	21	0.00	0.99

Design-level performance

SMF Designed for SDC D_{max}

Archetype	Repair		Prob. of Unsafe Placards	Resilience
	Cost ($)	Time (days)		
1-story				
MF	1,510,000	228	0.96	0.43
MF+GF	1,310,000	181	0.94	0.58
2-story				
MF	1,540,000	137	0.87	0.75
MF+GF	1,560,000	142	0.87	0.74
4-story				
MF	2,585,714	148	0.93	0.72
MF+GF	2,388,889	139	0.88	0.76
8-story				
MF	4,100,000	162	0.87	0.73
MF+GF	3,800,000	156	0.85	0.75

Design-level performance

SMF Designed for SDC D_{max}

Archetype	Repair Cost ($)	Repair Time (days)	Prob. of Unsafe Placards	Resilience
1-story				
MF	1,510,000	228	0.96	0.43
MF+GF	1,310,000	181	0.94	0.58
2-story				
MF	1,540,000	137	0.87	0.75
MF+GF	1,560,000	142	0.87	0.74
4-story				
MF	2,585,714	148	0.93	0.72
MF+GF	2,388,889	139	0.88	0.76
8-story				
MF	4,100,000	162	0.87	0.73
MF+GF	3,800,000	156	0.85	0.75

Design-level performance

8-story SMF Designed for SDC D_{max}

- **Repair Costs**: Most repair costs were caused by damage to the gypsum wall partitions, as before, but there were other significant contributions to repair costs, such as bolted shear tab gravity connections, and unanchored chiller and air handling units. The reserve lateral strength from the gravity framing reduced repair costs by 13%.

- **Repair Time**: Repair time was dominated by gypsum wall partitions, but many other fragility performance groups were significant contributors. The reserve lateral strength from the gravity framing reduced the predicted mean repair time by 6 days (4%).

Design-level performance

8-story SMF Designed for SDC D_{max}

- **Unsafe placards**: Placarding was mostly caused due to the prefabricated steel stair systems without seismic joints, but there were several other components that contributed to the probability of unsafe placards. Reserve strength slightly reduced the probability, with most improvement in reducing placard associated with unbraced fire sprinkler water piping.

Resilience contour plots

$$R = \int_{t_0}^{t_c} [1 - Q(t)]dt$$

$$= 1 - \frac{1}{2}\left(\frac{C_{Repair} + P_{Placard}C_{Tenant}}{C_{Total}}\right)\left(\frac{t_{Repair}}{t_c}\right)$$

$$= 1 - LT/2$$

$$L = \frac{2(1 - R)}{T}$$

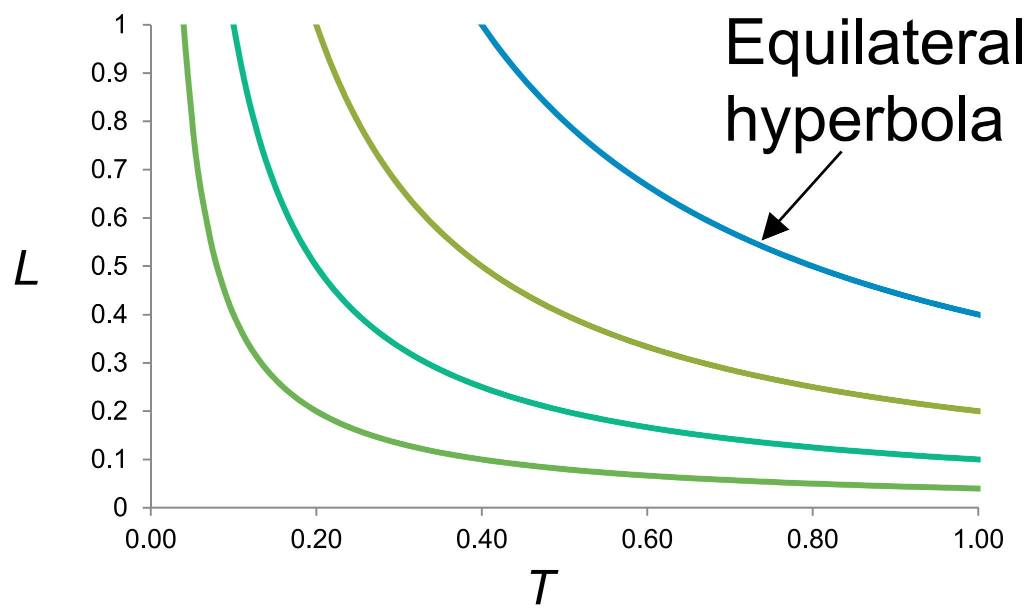

Serviceability-level resilience

Non-ductile Moment Frame

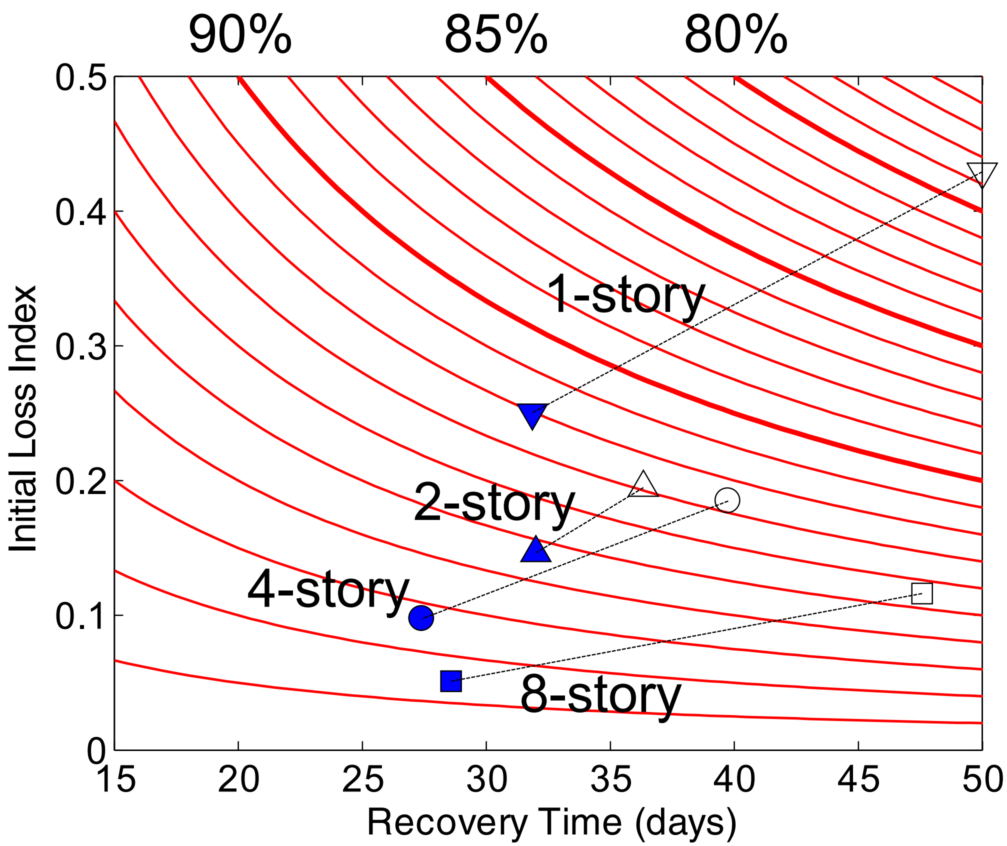

Serviceability-level resilience

SMF Designed for SDC D_{min}

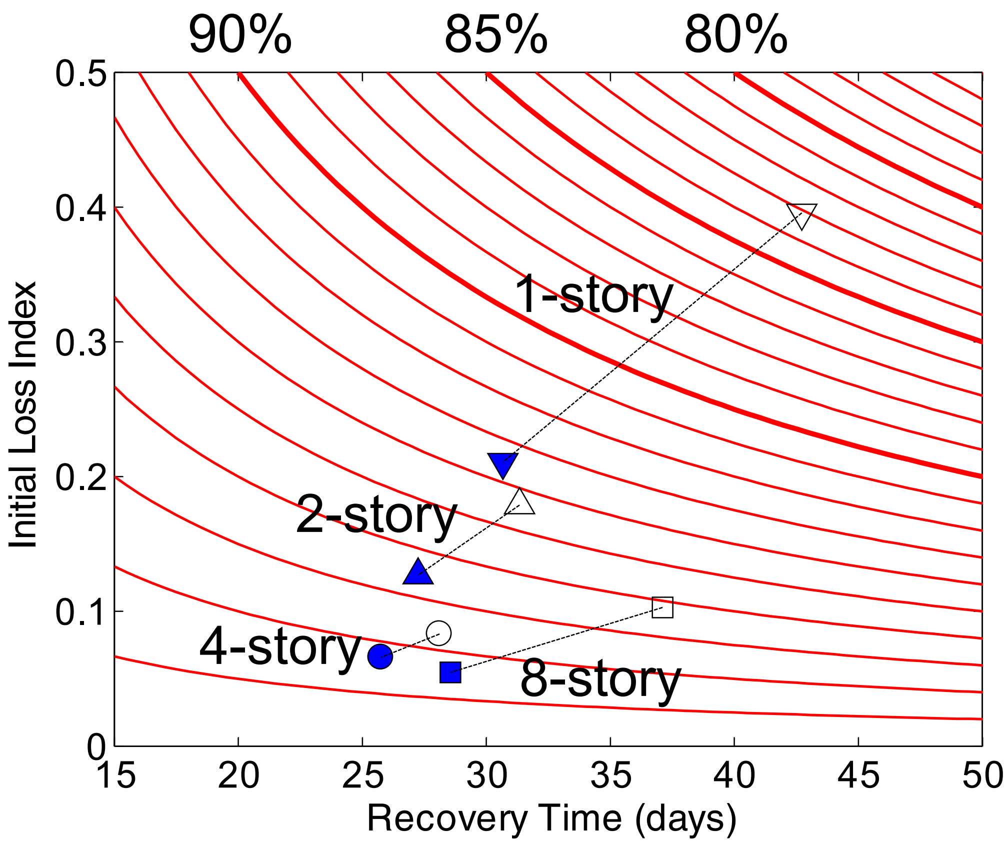

Serviceability-level resilience

SMF Designed for SDC D_{min}

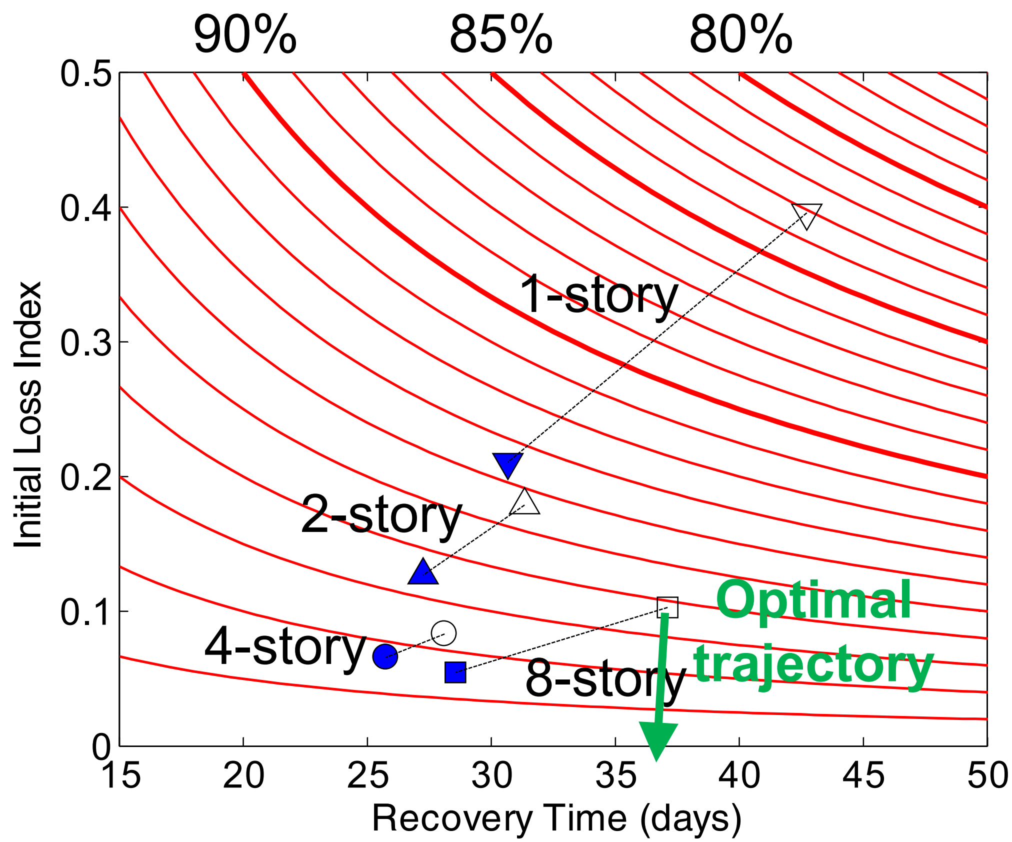

Target high-contributors (i.e. non-structural components) and note that optimal direction may not always be feasible to trace exactly.

Serviceability-level resilience

SMF Designed for SDC D_{max}

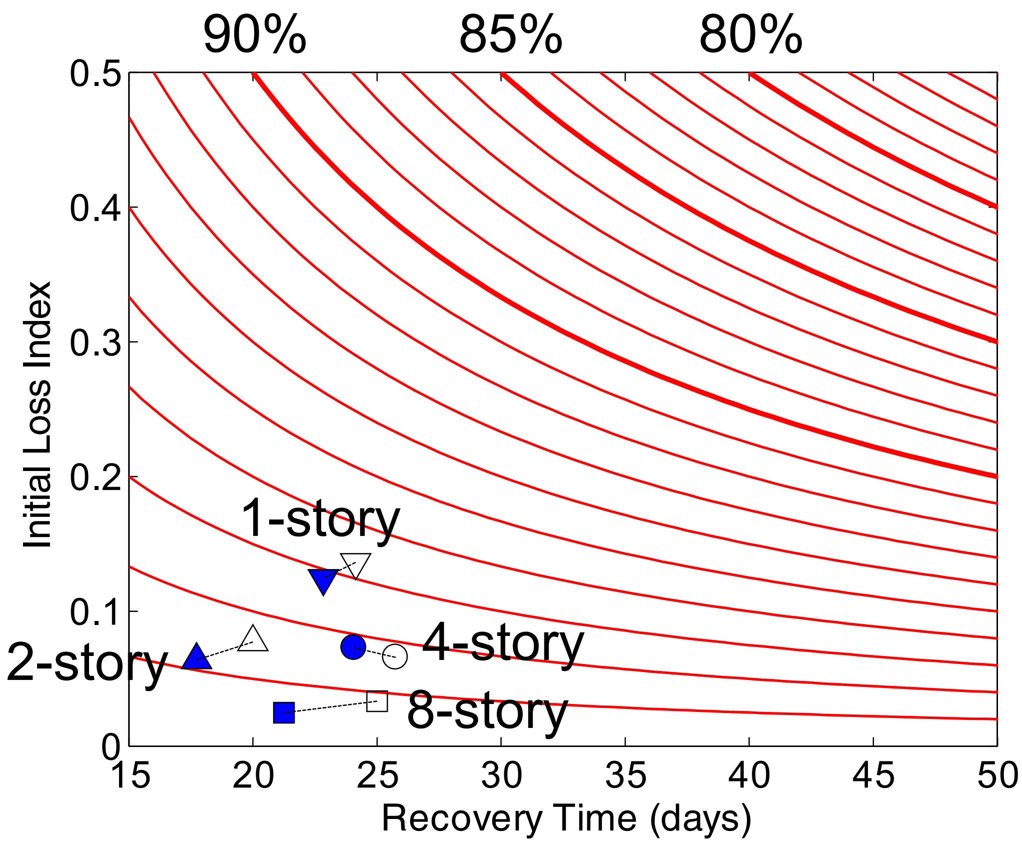

Design-level resilience

SMF Designed for SDC Dmax

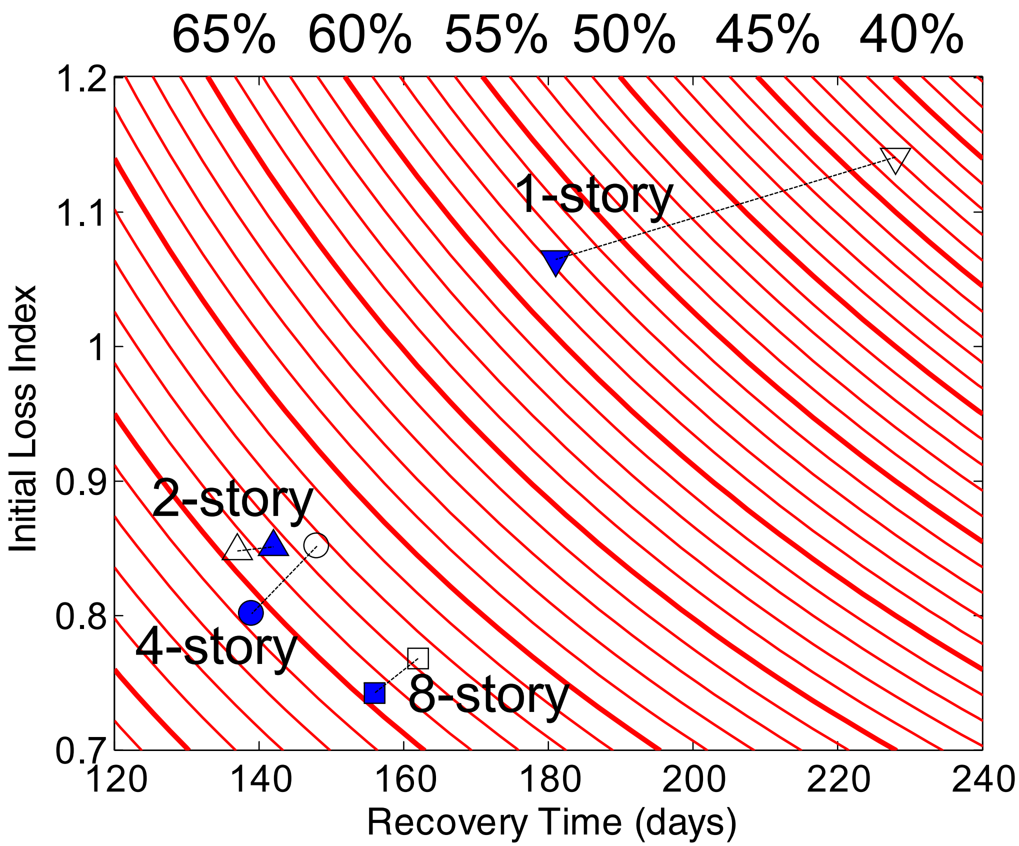

Design-level resilience

SMF Designed for SDC Dmax

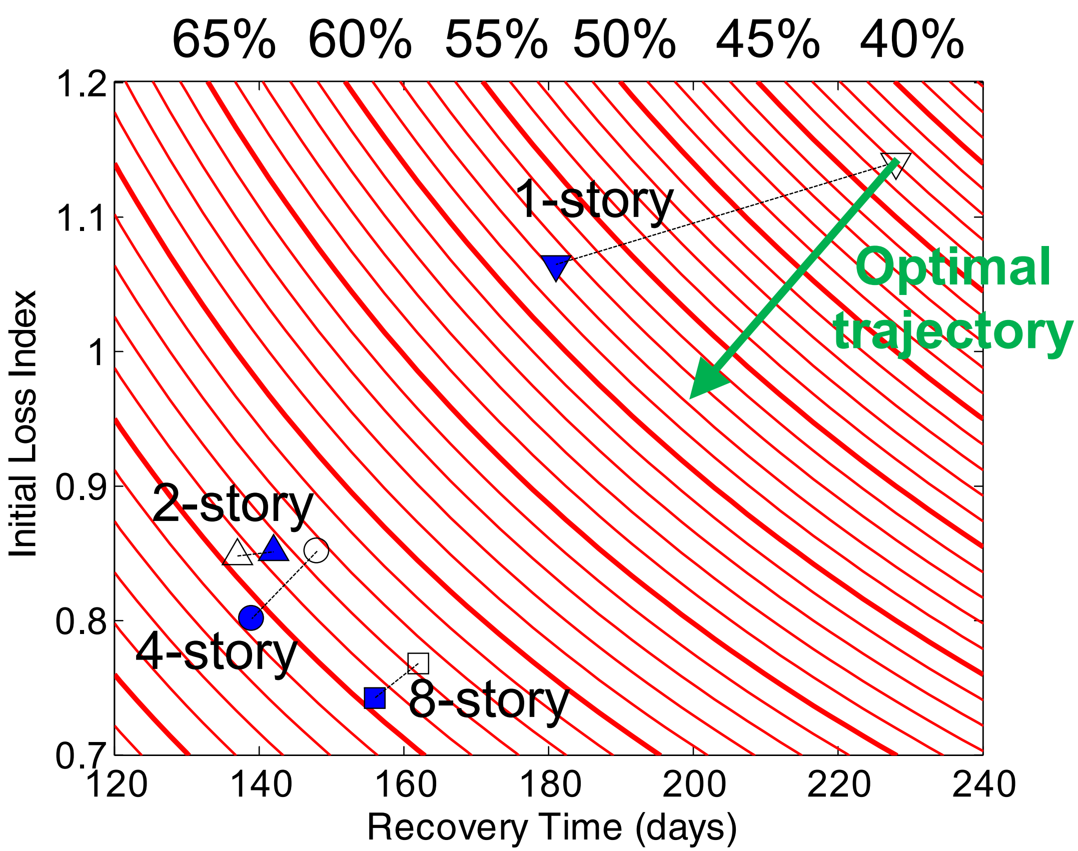

Serviceability-level resilience

SMF Designed for SDC D_{min}

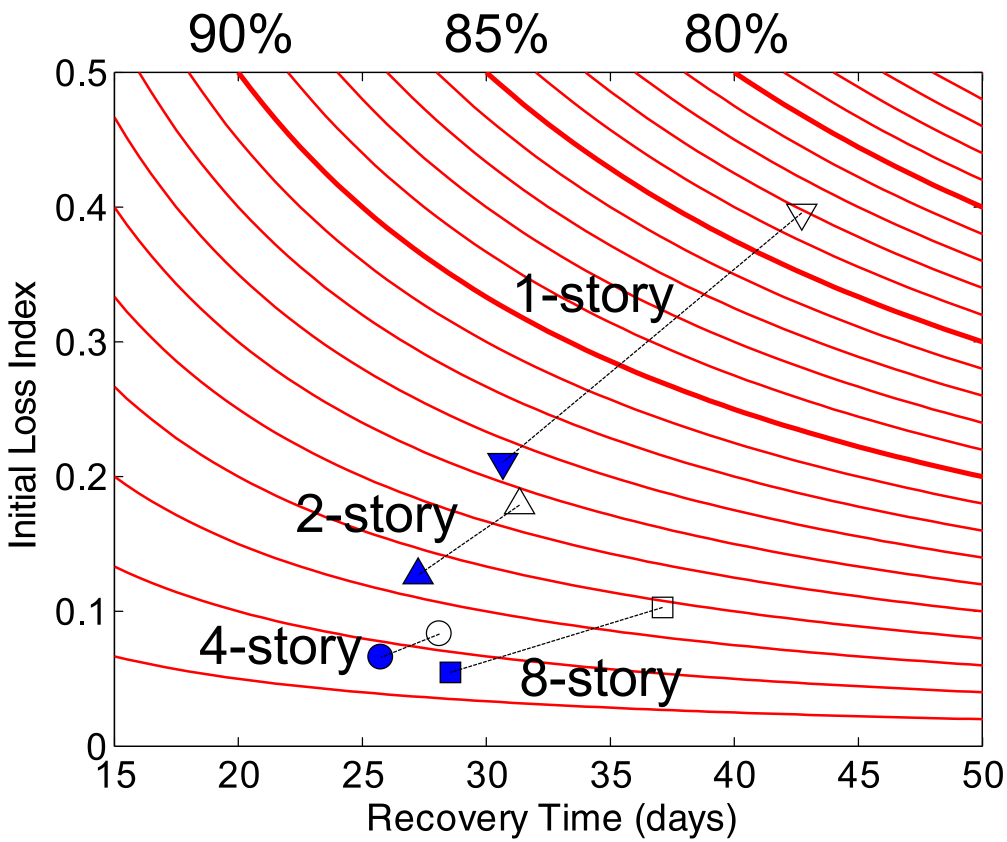

Conclusions

Reserve Strength Reserve lateral strength provided by shear tab connections was generally a significant factor in improving resilience, especially for archetype buildings with non-ductile moment frames or SMF designed for SDC D_{min}.

Resiliency Contour Plots Useful to visualize the tradeoff between improving robustness (reducing loss) and speeding recovery time, and to identify optimal path for developing resilience.

References

Bruneau, M., and Reinhorn, A., 2007, “Exploring the concept of seismic resilience for acute care facilities,” *Earthquake Spectra*, 23(1), 41–62.

Cimellaro, G.P., Reinhorn, A.M., and Bruneau, M., 2010, “Framework for analytical quantification of disaster resilience,” *Engineering Structures*, 32(11), 3639–3649.

Eatherton, M.R., and Hajjar, J.F., 2011, “Residual drifts of self-centering systems including effects of ambient building resistance,” *Earthquake Spectra*, 27(3), 719–744.

Flores, F.X., Charney, F.A., and Lopez-Garcia, D., 2014, “Influence of the gravity framing system on the collapse performance of special steel moment frames,” *Journal of Construction Steel Research*, 101, 351–362.

Hamburger, R.O., Krawinkler, H., Malley, J.O., and Adan, S.M., 2009, “Seismic design of steel special moment frames: a guide for practicing engineers,” NEHRP Seismic Design Technical Brief No. 2, produced by the NEHRP Consultants Joint Venture, a partnership of the Applied Technology Council and the Consortium of Universities for Research in Earthquake Engineering, for the National Institute of Standards and Technology, Gaithersburg, Maryland, NIST GCR 09-917-3.

Jarrett, J.A., Judd, J.P., and Charney, F.A., 2015, “Comparative evaluation of innovative and traditional seismic-resisting systems using the FEMA P-58 procedure,” *Journal of Constructional Steel Research*, 105, 107–118.

Judd, J.P., and Charney, F.A., 2014a, “Seismic performance of buildings designed for wind,” *Proceedings*, 45th Structures Congress, American Society of Civil Engineers, April 3–5, Boston, Massachusetts.

Judd, J.P., and Charney, F.A., 2014b, “Seismic collapse prevention systems,” *Proceedings*, 10th National Conference on Earthquake Engineering (NCEE), Earthquake Engineering Research Institute, July 21–25, Anchorage, Alaska.

Judd, J.P., and Charney, F.A., 2014c, “Performance-based design in the central and eastern United States,” *Proceedings*, 45th Structures Congress, American Society of Civil Engineers, April 3–5, Boston, Massachusetts.

Leon, R.T., 1998, “Composite connections,” *Progress in Structural Engineering and Materials*, 1(2), 159-169.

Liu, J., and Astaneh-Asl, A., 2000, “Cyclic testing of simple connections including effects of slab,” *Journal of Structural Engineering*, 126(1), 32–39.

Liu, J., and Astaneh-Asl, A., 2004, “Moment-rotation parameters for composite shear tab connections,” *Journal of Structural Engineering*, 130(9), 1371-1380.

Lignos, D.G., and Krawinkler, H., 2011, “Deterioration modeling of steel components in support of collapse prediction of steel moment frames under earthquake loading,” *Journal of Structural Engineering*, 137 (11), 1291–1302.

Lowes, L.N., Mitra, N., and Altoonash, A., 2004, “A beam-column joint model for simulating the earthquake response of reinforced concrete frames,” *PEER Report 2003/10*, Pacific Earthquake Engineering Research Center, University of California, Berkeley, California.

PEER, 2012, *Open Systems for Earthquake Engineering Simulation (OpenSees)*, version 2.4.0. Pacific Earthquake Engineering Research Center, University of California, Berkeley, California.

Wen, R., Akbas, B., and Shen, J., 2013, “Practical moment–rotation relations of steel shear tab connections,” *Journal of Constructional Steel Research*, 88, 296–308.

Zobel, C.W., and Khansa, L., 2014, “Characterizing multi-event disaster resilience,” *Computers and Operations Research*, 42, 83-94.